

Direct electrochemistry of hemoglobin on graphene/Fe₃O₄ nanocomposite-modified glass carbon electrode and its sensitive detection for hydrogen peroxide

Yuqiao Wang · Huijun Zhang · Dan Yao · Junjie Pu · Yuan Zhang · Xiaorui Gao · Yueming Sun

Received: 9 August 2012 / Revised: 1 November 2012 / Accepted: 3 November 2012 / Published online: 16 November 2012
© The Author(s). This article is published with open access at Springerlink.com 2012

Abstract Graphene/Fe₃O₄ nanocomposite was prepared for the immobilization of hemoglobin (Hb) to improve the electron transfer between Hb and glass carbon electrode (GCE). The characterization of nanocomposites was described by transmission electron microscopy, Fourier transform infrared, Raman spectroscopy, and X-ray photoelectron spectroscopy, respectively. The electrochemistry of Hb on the graphene/Fe₃O₄-based GCE was investigated by cyclic voltammetry and amperometric measurement. The modified electrode showed a wide linear range from 0.25 μmol/L to 1.7 mmol/L with a correlation coefficient of 0.9967. The detection limit of the H₂O₂ biosensor was estimated at 6.0 × 10⁻⁶ mol/L at a signal-to-noise ratio of 3.

Keyword Direct electrochemistry · Nanocomposite · Sensitive detection · Hydrogen peroxide

Introduction

Graphene (GE), with one-atom-thick planar sheets of sp²-bonded carbon atoms, has attracted much attention recently due to its high surface area, excellent electrical conductivity,

good mechanical strength, and high thermal conductivity [1]. Based on these properties, GE has shown great potential applications in electronic devices [2], energy conversion and storage [3], and biosensors [4]. However, GE is limited to designing biosensors for its hydrophobicity and agglomerate in water [5, 6]. Therefore, the combination of GE with other functional materials may result in the composition integrating characterizations and functions of each component. Among these, poly(diallyldimethylammonium chloride) (PDDA), a linear positively charged polyelectrolyte, is an effective reducing agent and can prevent the aggregation of GE sheets through electrostatic repulsion [7, 8]. Fe₃O₄ with low toxicity, good biocompatibility, and strong adsorption ability may serve as an ideal matrix for investigating entrapped biomolecules. For these biomolecules, hemoglobin (Hb) is a heme protein containing four electroactive iron hemes, which can store and transport oxygen in red blood cells [9]. In contrast to most other proteins, Hb is highly stable and can construct H₂O₂ sensor as a result of its commercial availability and peroxidase activity [10]. However, it is difficult for an electron to transfer between Hb and the electrode, as the redox center of proteins is embedded in polypeptide chain structures. The objective of this work was to explore the ability of the GE/Fe₃O₄ nanocomposite in immobilizing Hb on the electrode surface and promoting direct electron transfer between Hb and electrodes.

In this paper, we prepared Fe₃O₄ and then added it to the reduction process, during which process the graphene oxide was reduced to GE by PDDA. The GE/Fe₃O₄ nanocomposite was modified onto a glass carbon electrode (GCE), where Hb was immobilized by drop casting. The amperometric H₂O₂ biosensor based on GE/Fe₃O₄/Hb GCE was fabricated for investigating the effect of the nanocomposite on the direct electrochemistry of Hb, including the linear range, detection limitation, solution pH, stability, and reproducibility towards H₂O₂.

Y. Wang (✉) · H. Zhang · D. Yao · J. Pu · Y. Sun
School of Chemistry and Chemical Engineering,
Southeast University,
Nanjing 211189, China
e-mail: yqwang@seu.edu.cn

Y. Zhang
School of Chemistry and Chemical Engineering,
Yangzhou University,
Yangzhou 225002, China

X. Gao
School of Science, Hebei University of Engineering,
Handan 056038, China

Experimental

Reagents

Graphite powder (325 mesh) was obtained from Nanjing XF Nano Materials Tech Co., Ltd. PDDA (Mw, $2\text{--}3.5 \times 10^5$), Hb (Mw, 64,500), chitosan (Mw, $5\text{--}6 \times 10^5$, >85 % deacetylation), diethanolamine (DEA), and diethylene glycol (DEG) were purchased from Sigma. All other chemicals were of analytical reagent grade. The phosphate buffer solution (PBS, 0.1 mol/L) and the doubly distilled water were used in all the experiments unless otherwise stated.

Apparatus and measurements

Transmission electron microscopy (TEM) was carried out with Tecnai 12 operating at 200 kV accelerating voltage. Fourier transform infrared (FTIR) was recorded by Bruker Vector with the KBr method. Raman spectra were collected on Horiba-JY HR 800 equipped with a 514.5-nm laser source. X-ray photoelectron spectroscopy (XPS) was performed using Thermo Scientific ESCALAB 250 equipped with Mg $K\alpha$ radiation ($h\nu=1,253.6$ eV) at a power of 250 W. Cyclic voltammetry (CV) and amperometric measurement were carried out on CHI760D electrochemical workstation using three electrode systems. The working electrode was GCE (3 mm in diameter) and modified GCE. A saturated calomel electrode and a platinum wire served as reference and counter electrodes, respectively. All tested solutions were purged with N_2 before experiments and during measurements. In the electrochemical testing and analysis, the abbreviated symbols are explained as follows: anodic and cathodic voltage ($E_{p,a}$ and $E_{p,c}$), anodic and cathodic current ($I_{p,a}$ and $I_{p,c}$), and correlation coefficient (R_n).

Preparation of GE/Fe₃O₄ nanocomposite

Firstly, Fe₃O₄ nanoparticles were synthesized by a solvothermal coprecipitation method [11, 12]. In brief, FeCl₃·6H₂O (10 mmol) and FeCl₂·4H₂O (5 mmol) were dispersed in DEG (50 mL) for 30 min at 90 °C. DEA (10 mL) was added to the above solution. Meanwhile, NaOH (40 mmol) and DEG (20 mL) were mixed to produce a stock solution and then introduced into the hot iron solution. The mixture was kept in a Teflon-lined autoclave for 8 h at 200 °C. After centrifugation and washing, Fe₃O₄ nanoparticles were obtained. Secondly, graphite oxide (GO) was prepared from graphite powder by a modified Hummers method [13]. Under ultrasonic irradiation, GO (100 mg) was dispersed in deionized water (100 mL) to yield a yellow–brown dispersion. The unexfoliated GO was removed by centrifugation. Subsequently, the homogeneous GO dispersion was mixed with PDDA solution

(6 mL, 20 wt%) and Fe₃O₄ nanoparticles under vigorous stirring. When the suspension was maintained for 5 h in refluxing conditions, GE/Fe₃O₄ nanocomposite was obtained. If Fe₃O₄ was not added at the previous step, the PDDA-functionalized graphene (PDDA-G) was collected.

Configuration of modified electrode

The bare GCE was polished with 1.0, 0.3, and 0.05 μm alumina slurry, rinsed thoroughly with deionized water, and dried by N_2 blowing. Each of GE/Fe₃O₄, PDDA-G, and Fe₃O₄ of 1.5 mg was added into 1 mL 0.5 % chitosan solution to form different suspending mixtures under ultrasonication for 2 h. The various suspensions of 5 μL were cast onto the surface of GCE or modified GCE and then dried at room temperature. The GE/Fe₃O₄/Hb-, PDDA-G/Hb-, and Fe₃O₄/Hb-modified electrodes were prepared by the simple drop-casting technique in a Hb solution of 5 mg/L.

Results and discussion

Characterization of GE/Fe₃O₄

The morphology of GE/Fe₃O₄ was observed by TEM. Figure 1a shows GO has been reduced to GE sheet by PDDA, clarifying the crumpled and wrinkled flake-like structure. Adding Fe₃O₄ to GO reducing reaction, Fe₃O₄ nanoparticles adhere uniformly to the surface of an individual GE sheet with little Fe₃O₄ agglomeration in Fig. 1b. As shown in Fig. 1c, the Fe₃O₄ particle diameter is roughly 7 nm, providing a catalytic reaction active center.

As shown in Fig. 2, FTIR was employed to confirm the chemistry structure of the GE/Fe₃O₄ nanocomposite and the functionalized and assembly process. For GE/Fe₃O₄, the peaks at 632 and 580 cm⁻¹ are denoted to stretching vibrations of Fe–O, which suggests the presence of iron oxide. Compared with GO, the absorption intensities of GE/Fe₃O₄ at 960, 1,110, 1,395, and 1,733 cm⁻¹ decrease or even disappear. These bands can be attributed to ether/ester (C–O–C), alkoxy (C–O), carboxy (C=O), and carbonyl/carboxy (C=O) groups, respectively. The results prove that the oxygen functional groups of GO are almost entirely removed from GE with PDDA acting as reducing reagent. Simultaneously, PDDA-G owns the characteristic bands of PDDA at 2,921 (CH_n), 1,630 (C=C) and 1,465 (C=C), 1,381 (N–O), and 862 cm⁻¹ (C–N), which suggests the GE is successfully functionalized by PDDA.

Raman spectroscopy was used to probe the disorder of carbon structures during the change from graphite to GO and GE. Figure 3 shows the typical D band (~1,350 cm⁻¹) and G band (~1,580 cm⁻¹) of graphite. The D band is

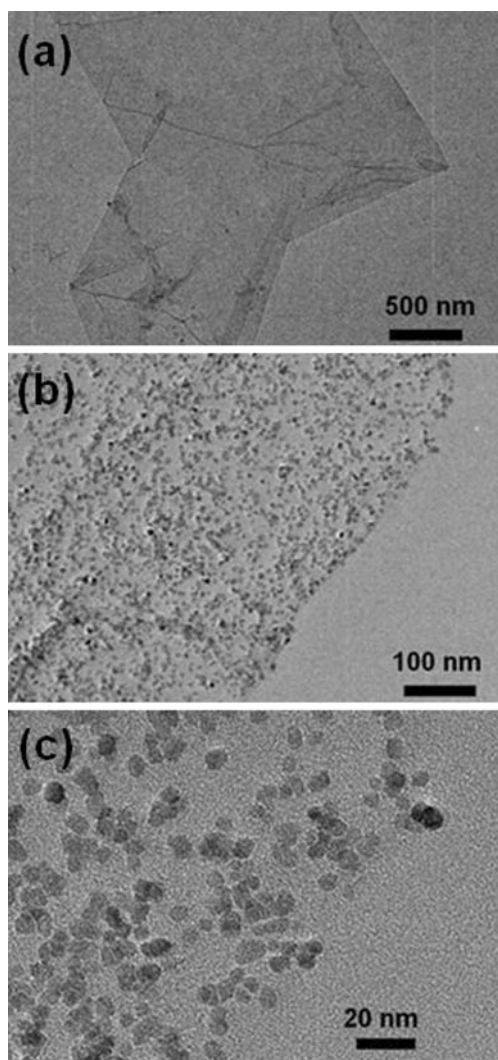


Fig. 1 TEM image of **a** GE, **b** GE/Fe₃O₄, and **c** zoomed-in edge of **b**

assigned to the vibrations of sp³ carbon atoms of disordered graphite. The G band is related to the coplanar vibration of sp² carbon atoms in a 2D hexagonal lattice. Generally, the intensity ratio of the D to G band (I_D/I_G) is a useful indicator to evaluate the ordered and disordered crystal structures of carbon. The I_D/I_G value of 0.28 for graphite is very small, reflecting the low defect density of graphite. Then, the value increases to 1.56 for GO, indicating the presence of some defects for GO in the oxidative process. The I_D/I_G value of 2.34 for GE/Fe₃O₄ suggests that the PDDA assistant reducing reaction decreases sp² graphitic domains and increases edge planes and disordered structures in GE sheets.

The surface chemical states of GO, PDDA-G, and GE/Fe₃O₄ were discussed by XPS. Figure 4a shows the N1s peak was visible in PDDA-G, which implied the strong interaction between PDDA and GE. If Fe₃O₄ was added to the procedure of PDDA-functionalized GE, Fe₃O₄ became the part of the homogeneous PDDA-functionalized GE/

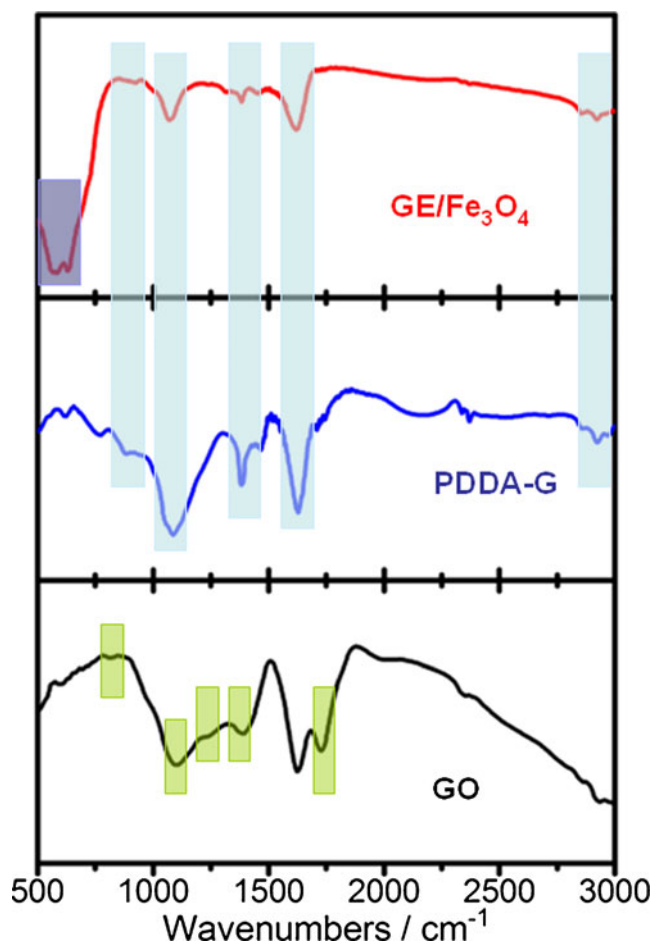


Fig. 2 FTIR spectra of GO, PDDA-G, and GE/Fe₃O₄

Fe₃O₄ composite. This process was confirmed by the Fe2p peak in GE/Fe₃O₄. For the C1s spectrum of Fig. 4b and c, the calculated oxygen content reduced from 28 to 17 %, indicating GO being effectively reduced to GE. Furthermore, the

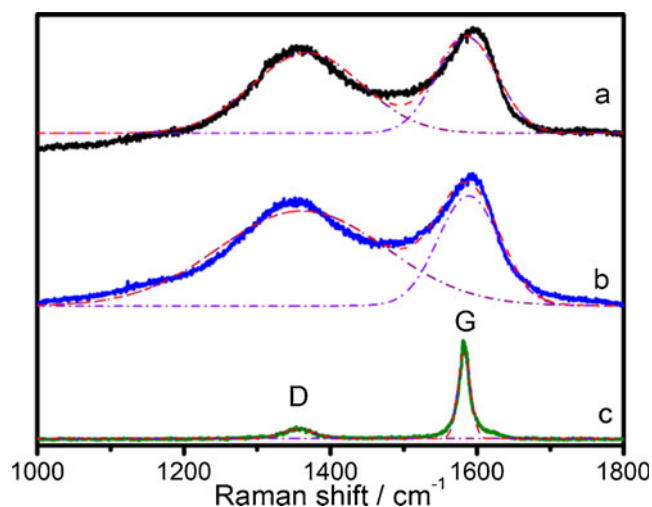


Fig. 3 Raman spectra of **a** GE/Fe₃O₄, **b** GO, and **c** graphite

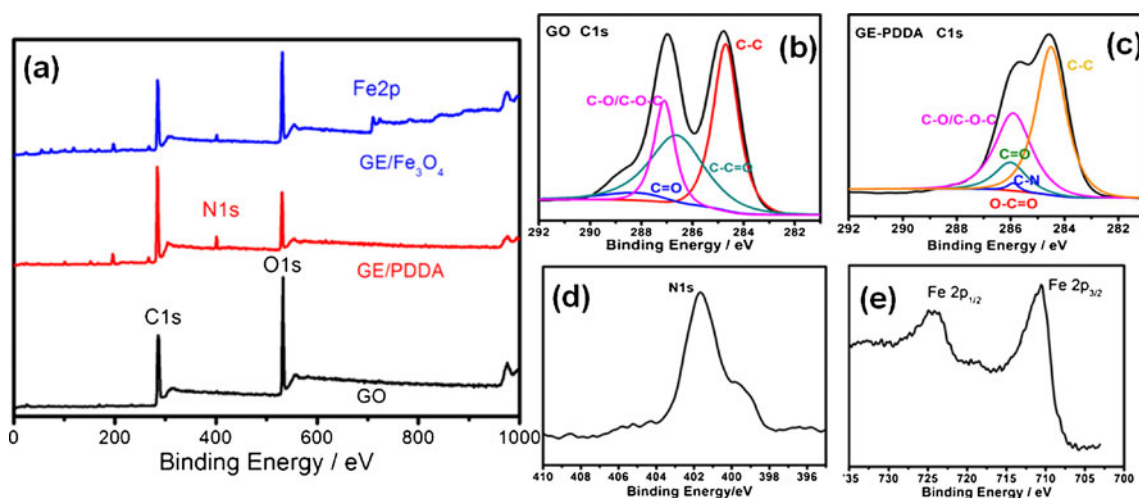


Fig. 4 XPS spectra of GO, PDDA-G, and GE/Fe₃O₄: **a** survey scan, high-resolution scan in the **b** C1s region of GO, **c** C1s, and **d** N1s regions of PDDA-G and **e** Fe2p region of GE/Fe₃O₄

binding energy peaks at 285.9, 711.8, and 725.1 eV in Fig. 4d and e, corresponding to the N1s, Fe 2p_{3/2}, and Fe 2p_{1/2}, respectively. The disappearance of the charge transfer satellite of Fe 2p_{3/2} around 720 eV reveals the formation of mixed oxides of Fe(II) and Fe(III) such as Fe₃O₄.

Direct electrochemistry of Hb

The direct electrochemistry of Hb-modified electrodes was recorded by CV. The specific peak was observed at PDDA-G/Hb/GCE and Fe₃O₄/Hb/GCE in Fig. 5a, indicating the

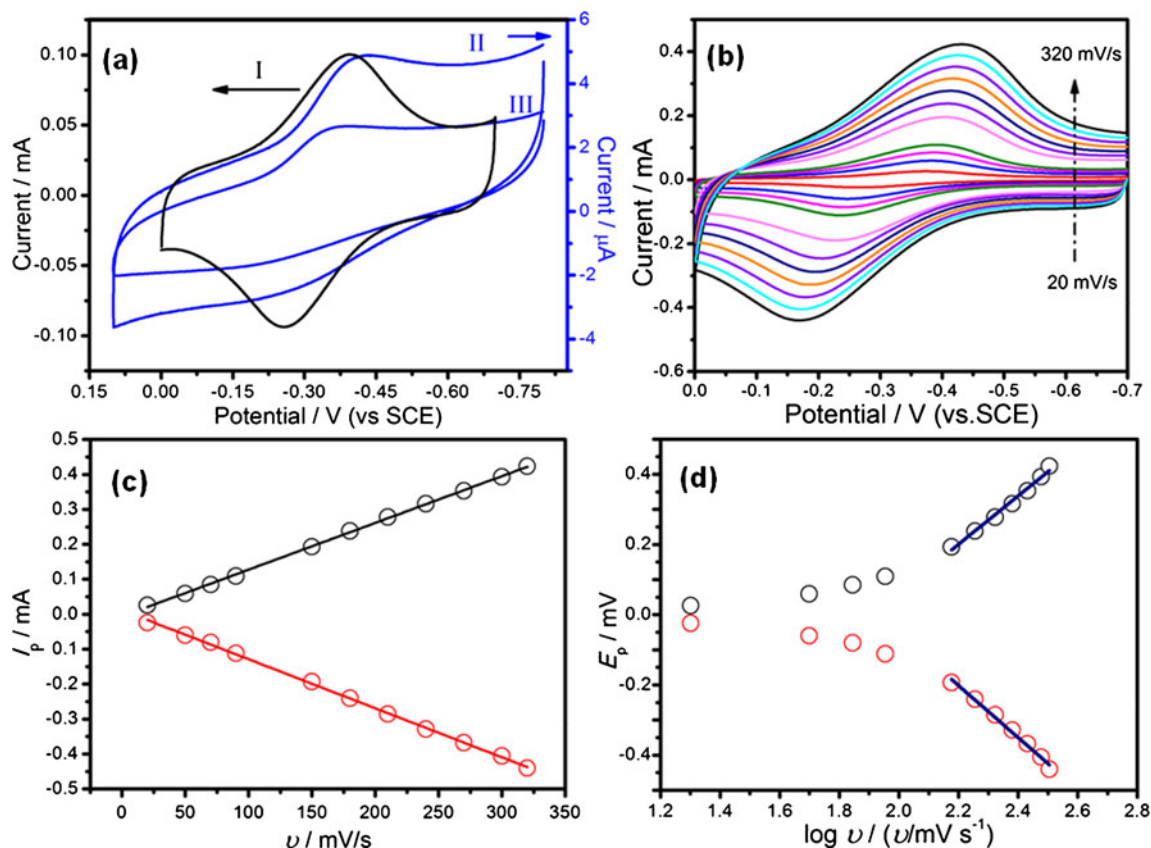


Fig. 5 CV plots of **a** (I) GE/Fe₃O₄/Hb-, (II) PDDA-G/Hb-, and (III) Fe₃O₄/Hb-modified GCE at the scan rate of 100 mV/s, **b** GE/Fe₃O₄/Hb-modified GCE with different scan rates (20, 50, 70, 90, 150, 180,

210, 240, 270, 300, and 320 mV/s), **c** the linear dependence of anodic and cathodic peak currents on scan rate (20 to 320 mV/s), **d** variation of E_p versus the logarithm of scan rates

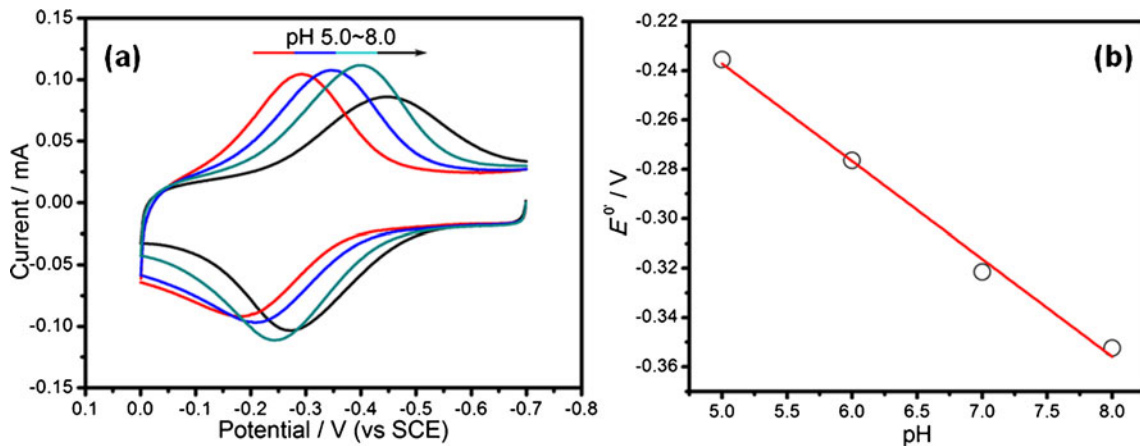


Fig. 6 **a** CV plots of the Hb immobilized on GE/Fe₃O₄/GCE in 0.2 mol/L PBS at different pH values with scan rate of 100 mV/s, **b** effect of pH on $E^{0'}$

electro-inactiveness of PDDA-G/Hb and Fe₃O₄/Hb. However, a pair of well-defined and quasi-reversible redox peaks GE/Fe₃O₄/Hb/GCE was observed at -0.394 and -0.255 V with a peak-to-peak separation value ($\Delta E_p = |E_{p,a} - E_{p,c}|$) of about 139 mV, revealing the direct electron transfer reaction. The formal potential ($E^{0'} = \frac{E_{p,a} + E_{p,c}}{2}$) is -0.324 V in PBS, which indicates that the redox reactions are associated with the reduction/oxidation of the HbFe(III)/Fe(II) couple [14]. The cathodic and anodic peak currents were located at -0.09367 and -0.1002 mA, respectively. The peak current ratio is about 1.0, indicating that the direct electron transfer process is a stable and reversible electron transfer reaction. Figure 5b shows the scan rate effects on both the peak voltage and current. As the scan rate increases from 20 to 320 mV/s, both $I_{p,a}$ and $I_{p,c}$ can be described by the linear regression equations as $I_{p,a} = 0.00134v - 0.00618$ ($R_n=0.9994$) and $I_{p,c} = -0.0014v + 0.0117$ ($R_n=0.9991$) in Fig. 5c. The linear changing suggests that the redox of Hb

on the GE/Fe₃O₄/GCE is a quasi-reversible surface-controlled electrochemical process. Similarly, both $E_{p,a}$ and $E_{p,c}$ shift slightly with increasing scan rate, resulting in the increment of the peak-to-peak separation. The electrochemical parameters were calculated according to Laviron equations [15]:

$$E_{p,a} = E^{0'} + \frac{2.3RT}{(1-\alpha)nF} \log v \tag{1}$$

$$E_{p,c} = E^{0'} - \frac{2.3RT}{\alpha nF} \log v \tag{2}$$

$$\log k_s = \alpha \log(1-\alpha) - (1-\alpha) \log \alpha + \log \frac{RT}{nFv} - \frac{\alpha(1-\alpha)nF\Delta E_p}{2.3RT} \tag{3}$$

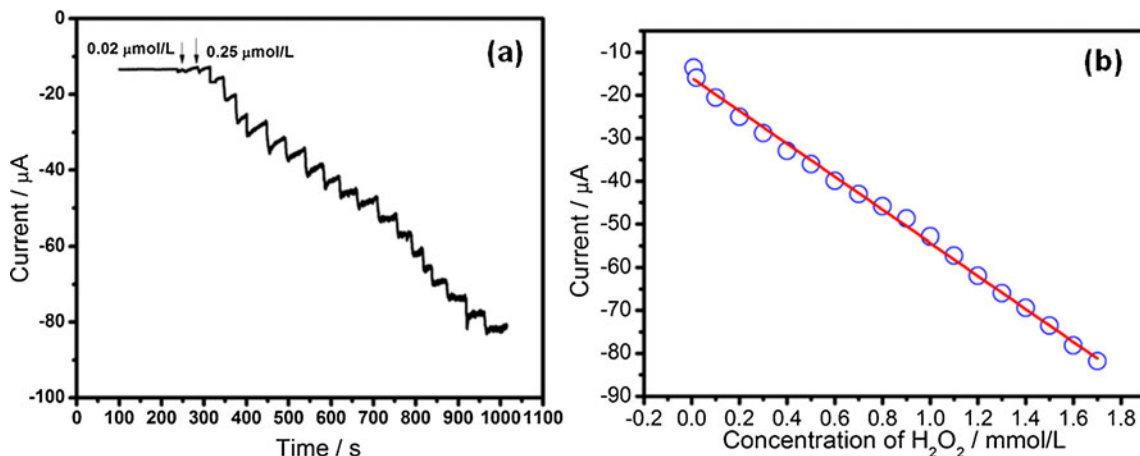
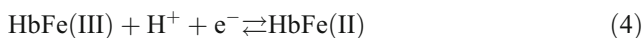


Fig. 7 **a** Amperometric responses of H₂O₂ upon successive addition of 20 μL H₂O₂ in N₂-saturated PBS, **b** the peak current versus H₂O₂ concentration

where α is the charge transfer coefficient, ν is the scan rate, n is the electron transfer number, k_s is the apparent charge transfer rate constant, R is the gas constant, and F is Faraday's constant. Figure 5d shows the linear relationship of E_p and $\log \nu (\nu/\text{mVs}^{-1})$ with the linear regression equations as $E_{p,a} = 0.1359 \log \nu - 0.5384$ ($R_n=0.9966$) and $E_{p,c} = -0.09629 \log \nu - 0.2143$ ($R_n=0.9840$). Obviously, the slopes of the linear segments are equal to $-2.3RT/\alpha nF$ and $2.3RT/(1-\alpha)nF$ for the $E_{p,c}$ and $E_{p,a}$ curves, respectively. The evaluated value of α and n is 0.58 and 1.05. According to the Eq. (3), k_s can be estimated to be 0.3 s^{-1} . The estimated k_s value is larger than that obtained for Hb immobilized on polymer-MWCNT-modified [9].

Effect of pH on the direct electrochemistry

The direct electrochemistry of Hb immobilized on GE/Fe₃O₄ showed a strong dependence on solution pH in Fig. 6a. The stable and well-defined CV plots were obtained, and E^0 showed a negative shift with the increase of buffer solution pH. The linear relationship of E^0 and the pH value was obtained from the linear regression equation as $E^0 = -0.0396\text{pH} - 0.0391$ ($R_n=0.9921$). The slope of -39.6 mV/pH is smaller than the expected theoretical value of 56 mV/pH at $20 \text{ }^\circ\text{C}$ for a single proton coupled to the reversible one-electron transfer [16]. It may be due to the influence of the protonization of ligands to the heme iron and amino acids around the heme [13]. Thus, the electron transfer between Hb and the electrode can be presented by:



Sensitive detection for H₂O₂

Considering the sensitivity and stability, the typical steady-state amperometric response of the biosensor is investigated by successively increasing the H₂O₂ concentration under the optimized conditions. Figure 7a shows a rapid current response with continuous addition of H₂O₂ to the testing solution. The maximum steady-state current could be achieved within 5 s, indicating a fast H₂O₂ diffusion process in the modified electrode due to the porous structure of the GE/Fe₃O₄ film. Figure 7b shows the calibration curve between amperometric current and H₂O₂ concentration. The regression equations were expressed as a linear equation $I_p = -0.3837c - 1.5954$ ($R_n=0.9967$). The detection limit of the biosensor was estimated at $6.0 \times 10^{-6} \text{ mol/L}$ at a signal-to-noise ratio of 3. The linear ranger is broader than that of the Hb/MCMS/GCE [9]. The result indicates that the magnetic microspheres in the experiment displayed

better catalytic ability than the microspheres using the magnetic core of carbon-coated iron nanoparticles.

Repeatability and stability of the H₂O₂ biosensor

Considering the fabrication repeatability of the biosensor based on the GE/Fe₃O₄/Hb GCE, five modified electrodes were prepared and measured independently. The relative standard deviation of peak currents was 2.3 % for measuring $25 \text{ } \mu\text{mol/L}$ H₂O₂ in PBS, revealing an excellent reproducibility. After the electrode was stored for 2 weeks at $4 \text{ }^\circ\text{C}$ in a humid environment, it could retain 95 % of its original response, suggesting acceptable storage stability.

Conclusion

In this work, the GE/Fe₃O₄ nanocomposite consisting of PDDA-functionalized GE covered with high-density Fe₃O₄ nanoparticles was prepared by a simple and cost-effective procedure. Then, the direct electrochemistry of Hb was investigated in detail by various electrochemical methods. The GE/Fe₃O₄/GCE showed a fast response on H₂O₂, a wide linear range, and a low detection limit towards H₂O₂. In addition, the fabricated H₂O₂ biosensor exhibited excellent reproducibility and stability. Based on these, a low-cost, highly efficient, and direct electrochemical method for H₂O₂ determination was developed.

Acknowledgments We gratefully acknowledge the financial support of the 973 Program (2013CB932902), National Natural Science Foundation of China (21173042), National Natural Science Foundation of Jiangsu (BK201123694) and Hebei (B2012402006), Jiangsu Key Laboratory of Environmental Material and Environmental Engineering (JHCG201012), and Foundation of Southeast of University (3212001102 and 3212002205).

Open Access This article is distributed under the terms of the Creative Commons Attribution License which permits any use, distribution, and reproduction in any medium, provided the original author(s) and the source are credited.

References

1. Novoselov KS, Geim AK, Morozov SV, Jiang D, Zhang Y, Dubonos SV, Grigorieva IV, Firsov AA (2004) Science 306:666–669
2. Biswas C, Lee Y (2011) Adv Funct Mater 21:3806–3826
3. Hou J, Shao Y, Ellis MW, Moore RB, Yi B (2011) Phys Chem Chem Phys 13:15384–15042
4. Shao Y, Wang J, Wu H, Liu J, Aksay IA, Lin Y (2010) Electroanal 22:1027–1036
5. He Y, Shen Q, Zheng J, Wang M, Liu B (2011) Electrochim Acta 56:2471–2476

6. Lu D, Zhang Y, Wang L, Lin SX, Wang CM, Chen XF (2012) *Talanta* 88:181–186
7. Zhang S, Shao Y, Liao H, Engelhard M, Yin G, Lin Y (2011) *ACS Nano* 5:1785–1791
8. Liu X, Zhu H, Yang XR (2011) *Talanta* 87:243–248
9. Tan XC, Zhang JL, Tan SW, Zhao DD, Huang ZW, Mi Y, Huang ZY (2009) *Sensors* 9:6185–6199
10. Yu CM, Zhou XH, Gu HY (2010) *Electrochim Acta* 55:8738–8743
11. Caruntu D, Caruntu G, Chen Y, O'Connor CJ, Goloverda G, Kolesnichenko VL (2004) *Chem Mater* 16:5527–5534
12. Chen M, Kim Y, Li C, Cho S (2008) *J Phys Chem C* 112:6710–6716
13. Li D, Müller M, Gilje S, Kaner R, Wallace GG (2008) *Nat Nanotechnol* 3:101–105
14. Liu H, Wan Y, Zou G (2006) *Anal Bioanal Chem* 385:1470–1476
15. Laviron E (1979) *J Electroanal Chem* 101:19–28
16. Sun W, Li X, Liu S, Jiao K (2009) *Bull Korean Chem Soc* 30:582–588